ЖЭТФ, 2006, том 130, вып. 1 (7), стр. 57–63

PAIR PRODUCTION BY A STRONG WAKEFIELD EXCITED BY LASERS IN A MAGNETIZED PLASMA

L. A. Rios [a]*, ***A. Serbeto*** [a], ***J. T. Mendonça*** [b], ***P. K. Shukla*** [b,c,d,e]**, ***R. Bingham*** [d,e]

[a] *Instituto de Física, Universidade Federal Fluminense*
24210-340, Rio de Janeiro, Brazil

[b] *GoLP, Centro de Física dos Plasmas, Instituto Superior Técnico*
1049-001, Lisboa, Portugal

[c] *Institut für Theoretische Physik IV, Ruhr-Universität Bochum*
D-44780, Bochum, Germany

[d] *Centre for Fundamental Physics, Rutherford Appleton Laboratory, Chilton, Didcot, Oxfordshire*
OX11 0QX, UK

[e] *Department of Physics, University of Strathclyde, Glasgow*
Scotland G4 0NG, UK

Received 10 January 2006

The production of electron–positron pairs due to accelerated electrons in a magnetized plasma is considered. The high-energy electrons are produced during laser–plasma interactions in the presence of spontaneously produced magnetic fields. By using a classical fluid description, we analyze the generation of electrostatic wakefields at the plasma wave-breaking limit and estimate the number of produced pairs for different situations. We note that in some cases, the presence of the magnetic field can increase the number of produced pairs.

PACS: 52.59.Rz, 12.20.-m, 52.38.-r, 52.35.Mw

1. INTRODUCTION

There are several mechanisms by which electron–positron pairs can be produced. One of the most popular mechanisms is the Schwinger pair production process [1], where pairs are spontaneously produced in a constant electric field if its strength in the vacuum exceeds the Schwinger critical value $E_{QED} = 1.3 \cdot 10^{16}$ V/cm. One possibility of pair production is by means of intense lasers, where electron–positron pairs can just «appear» from the vacuum in the focal region of the laser pulse (near the intensity 10^{29} W/cm^2, corresponding to the critical electric field). Many theoretical studies of the Schwinger mechanism using lasers have been made [3–6]. Narozhny et al. [6] considered the electron–positron pair production in an electromagnetic field created by two counterpropagating focused laser pulses, and showed that pair production can be experimentally observed when the intensity of each beam is close to 10^{26} W/cm^2, three orders of magnitude lower than that for a single pulse. However, the cross section for the Schwinger process at optical frequencies (or below) is so small at any laser intensity that this effect is insignificant [7].

Production of pairs is also possible in the Coulomb field of a nucleus via virtual photons («tridents»), which is a dominant energy-loss mechanism at high energies. In a trident process, high-energy electrons, whose kinetic energy exceeds the pair-production threshold $2m_ec^2$, can produce the electron–positron pairs by scattering in the Coulomb potential of a nucleus. Some authors [8, 9] presented a preliminary discussion about pair production by relativistic electrons accelerated by intense lasers, while others discussed pair production due to scattering of high-energy electrons produced in strong wakefields driven by ultra-intense short laser pulses [10] and neutrino beams [11]. Recently, Berezhiani et al. [12] performed

*E-mail: rios@if.uff.br
**E-mail: ps@tp4.ruhr-uni-bochum.de

simulations of laser pulse dynamics in overdense plasmas and showed that an intensive production of pairs by the driven motion of the plasma electrons occurs owing to a trident process.

The nonlinear interaction of lasers with plasmas can give rise to a large number of interesting phenomena. The latest advances in the pulse compression technique have provided the possibility of generating high-intensity laser pulses with the intensity I approaching 10^{20} W/cm^2 at the wavelength $\lambda \sim 1054$ nm (and the promise of an even higher intensity $I = 10^{24}$ W/cm^2). At such intensities, the electron motion in the laser field is essentially relativistic and the physics of the laser–plasma interactions is very different from the case of moderate intensities. Specifically, high-intensity laser pulses spontaneously create strong magnetic fields [13], whose effects should be considered in a realistic description of laser–plasma interactions and associated nonlinear phenomena.

In this paper, we present a theoretical investigation of the electron–positron pair production by the electrons accelerated due to laser–plasma interactions in a homogeneous magnetic field. Specifically, we consider the nonlinear interaction between an intense short laser pulse and a collisionless cold magnetoplasma, by assuming that the ions form a neutralizing background. The electrons can be directly accelerated by the intense laser or by the strong wakefields generated during the nonlinear laser–plasma interaction, and then produce pairs by scattering in the Coulomb potential of immobile ions. We use a classical fluid description to analyze this nonlinear interaction and determine the pair concentration produced by the electrons. Different laser intensities, pulse widths and directions of the external magnetic field are considered, and the electrostatic wakefield (at the wave-breaking limit) and the number of produced pairs in each case are analyzed.

The paper is organized as follows. The governing nonlinear equations for intense laser–plasma interactions in an external magnetic field are presented in Sec. 2. There, we focus on the generation of wakefields by arbitrary large-amplitude electromagnetic fields, and derive the relevant equations. The production of electron–positron pairs due to the accelerated electrons in the wakefields is discussed in Sec. 3. Numerical results for the wakefields and associated pairs are given in Sec. 4. Finally, Sec. 5 contains a brief summary and possible applications of our work to laboratory and astrophysical plasmas.

2. GOVERNING EQUATIONS

We consider a cold, collisionless, relativistic electron–ion plasma in the presence of intense circularly polarized electromagnetic (CPEM) waves and an external magnetic field. We study the nonlinear interaction between the CPEM waves and the magnetized plasma by using the equations

$$\frac{\partial N_\sigma}{\partial t} + \nabla \mathbf{\Gamma}_\sigma = 0, \tag{1}$$

$$\frac{\partial \mathbf{p}_\sigma}{\partial t} + (\mathbf{v}_\sigma \cdot \nabla)\mathbf{p}_\sigma = q_\sigma \left(\mathbf{E} + \frac{\mathbf{v}_\sigma}{c} \times \mathbf{B} \right), \tag{2}$$

$$\nabla \mathbf{E} = -4\pi e \left(N_e - N_i \right), \tag{3}$$

$$\nabla \times \mathbf{E} = -\frac{1}{c} \frac{\partial \mathbf{B}}{\partial t}, \tag{4}$$

$$\nabla \times \mathbf{B} = \sum_\sigma \frac{4\pi}{c} q_\sigma \mathbf{\Gamma}_\sigma + \frac{1}{c} \frac{\partial \mathbf{E}}{\partial t}, \tag{5}$$

and

$$\nabla \mathbf{B} = 0, \tag{6}$$

where

$$\mathbf{p}_\sigma = \gamma_\sigma m_\sigma \mathbf{v}_\sigma$$

is the relativistic momentum of the particle species σ (σ equals e for the electrons and i for the ions) and

$$\gamma_\sigma = 1/\sqrt{1 - v_\sigma^2/c^2}$$

is the relativistic Lorentz factor, m_σ is the rest mass, $\mathbf{v}_\sigma$ is the fluid velocity, c is the speed of light in vacuum,

$$\mathbf{\Gamma}_\sigma = N_\sigma \mathbf{v}_\sigma$$

is the particle flux, and N_σ is the number density of the species σ. Because we consider the generation of longitudinal (electrostatic) fields, the vector $\mathbf{B}$ includes only the wave magnetic field and the external magnetic field $\mathbf{B}_0$. Besides, we study the wakefield generation on timescales that are either comparable to or shorter than the electron plasma period ω_p^{-1}, and therefore collisions between electrons and ions are neglected (we consider

$$\omega_p \gg \nu,$$

where

$$\omega_p = \sqrt{\frac{4\pi N_0 e^2}{m_e}}$$

is the electron plasma frequency and ν the electron–ion collision frequency). Furthermore, on the fast timescales of the light pulse and rapid electron motions, the ions do not respond and can be considered immobile.

In what follows, we are concerned with the nonlinear propagation of a short laser pulse in a magnetized plasma. Assuming that the latter is transparent to the laser propagation, we can consider the pulse nonevolving and propagating at a constant velocity near the light speed. Thus, the laser vector potential

$$A = |\mathbf{A}|$$

is a function of the variable

$$\xi = z - v_g t,$$

where v_g is the group velocity of the laser in the plasma (we consider the laser is traveling from left to right). The scalar and vector potentials ϕ and $\mathbf{A}$ are defined as

$$\mathbf{E} = -\frac{1}{c}\frac{\partial \mathbf{A}}{\partial t} - \nabla\phi, \tag{7}$$

$$\mathbf{B} = \nabla \times \mathbf{A} + \mathbf{B}_0, \tag{8}$$

and

$$\nabla \cdot \mathbf{A} + \frac{1}{c}\frac{\partial \phi}{\partial t} = 0. \tag{9}$$

During the interaction of a laser pulse with the plasma electrons under nonrelativistic conditions, the pulse ponderomotive force creates a local charge separation, which gives rise to an electrostatic field. In general, this field remains after the laser pulse passes and its relaxation induces the electron wake oscillations with the phase speed near the speed of the light pulse ($v_\phi \approx v_g$) and a frequency near the plasma frequency ω_p [14].

In the nonrelativistic case, one expects that the efficiency of wakefield generation is highest if the laser pulse width d is half λ_p, the wavelength of the wake oscillations [14, 15]. On the other hand, if d is much smaller than this optimum value, the dynamics of the electrons can be completely dominated by the ponderomotive force, and the electrons are then trapped by the pulse. However, wake oscillations can still be excited, but they are much weaker than those in the optimum case.

As the laser intensity grows, the optimum pulse width becomes smaller and a much stronger charge field separation is created. In fact, the wake oscillations can be of an amplitude higher than that of the laser and become highly nonlinear. For intense laser fields, the plasma electrons can acquire relativistic velocities. Consequently, a nonlinear current is produced that gives rise to a modification of the linear dispersion relation. Owing to this and other nonlinear effects, the wave can propagate through an overdense region because its frequency ω becomes larger than ω_p.

If the wave pulse is circularly polarized, the normalized vector potential

$$\mathbf{a} = \frac{e\mathbf{A}}{m_e c^2}$$

can be written in the form

$$\mathbf{a} = a\left(\hat{x}\cos\chi + \hat{y}\sin\chi\right), \tag{10}$$

where

$$\chi = k_p(z - v_g t),$$

with $v_g \approx v_\phi$ and $k_p = 2\pi/\lambda_p$. For a Gaussian pulse, a^2 is given by

$$a^2 = a_0^2 \exp\left(-\frac{\chi^2}{k_p^2 L^2}\right), \tag{11}$$

with $L = d/2$. In practical units, $a_0 = 0.85 \cdot 10^{-9}\lambda\sqrt{I}$, where I is the intensity of the laser in W/cm^2 and λ is the wavelength of the laser light in microns [16].

Normalizing all the physical quantities, writing them as functions of the variable χ (plane waves), and considering that the longitudinal plasma waves are propagating along the z-direction, we obtain the set of final equations from Eqs. (1)–(11) as

$$\left[\hat{z}\cdot\mathbf{P}_e - \beta_\phi\sqrt{1+P_e^2}\right]\frac{d\mathbf{P}_e}{d\chi} = \\ = \sqrt{1+P_e^2}\left(\frac{d\Psi}{d\chi}\hat{z} - \beta_\phi\frac{d\mathbf{a}}{d\chi}\right) + \\ + (\hat{z}\times\mathbf{P}_e)\times\frac{d\mathbf{a}}{d\chi} + \frac{\beta_\phi}{\omega_p}\mathbf{\Omega}\times\mathbf{P}_e, \tag{12}$$

and

$$\frac{d^2\Psi}{d\chi^2} = \beta_\phi^2\left[\frac{\Gamma_e\sqrt{1+P_e^2}}{\hat{z}\cdot\mathbf{P}_e - \beta_\phi\sqrt{1+P_e^2}} - 1\right], \tag{13}$$

where

$$\Gamma_e = \frac{\hat{z}\cdot\mathbf{P}_{e0} - \beta_\phi\sqrt{1+P_{e0}^2}}{\sqrt{1+P_{e0}^2}}$$

is a constant that depends on the initial value of the normalized electron momentum

$$\mathbf{P}_e = \frac{\mathbf{p}_e}{m_e c}.$$

Here,

$$\Psi = \frac{e\phi}{m_e c^2}$$

is the normalized scalar potential,

$$\beta_\phi = \frac{v_\phi}{c}$$

is the normalized phase speed, and

$$\mathbf{\Omega} = \frac{e\mathbf{B}_0}{m_e c}$$

is the vector associated with the electron gyrofrequency,

$$\omega_c = \frac{eB_0}{m_e c}.$$

Equations (12) and (13) form a set of nonlinear equations for studying the generation of plasma waves during the laser–plasma interaction for different laser intensities (a_0), pulse widths (d), and directions of the external magnetic field ($\mathbf{\Omega}$). We note that Eq. (13) is a generalized Poisson equation written in a moving frame. Thus, the normalized electron plasma density in this frame is given by

$$\frac{N_e}{N_0} = \frac{\Gamma_e \sqrt{1+P_e^2}}{\hat{z}\cdot\mathbf{P}_e - \beta_\phi \sqrt{1+P_e^2}}. \qquad (14)$$

3. PAIR PRODUCTION

Assuming that each electron accelerated in the wakefield and scattered on the ions produces a pair, we can determine the electron–positron pair concentration n_p produced via the Bhabha trident process from the fraction of scattered electrons, i.e., [10]

$$\frac{dn_p}{dt} = \sigma_T N_i N_e v_e, \qquad (15)$$

where N_e and N_i are the electron and ion concentrations, v_e is the electron speed, and σ_T is the total cross section for the trident pair production process [17]. Because we assume that each scattered electron produces a pair, we consider these particles to be accelerated to relativistic energies (high γ_e values) and to reach the pair production threshold $2m_e c^2$. For large values of the Lorentz factor, the cross section σ_T can be written as [10, 12, 17]

$$\sigma_T = \frac{28}{27\pi}\left(\frac{Zr_0}{137}\right)^2 (\ln\gamma_e)^3, \qquad (16)$$

where $r_0 = 2.8\cdot 10^{-13}$ cm is the classical electron radius and Z is the ion nuclear charge. We note that expression (16) for the cross section has been derived in the absence of an external magnetic field; however, it does remain approximately valid for a magnetized plasma as long as

$$\hbar\omega_c \ll 2m_e c^2.$$

To determine pair concentrations, we rewrite Eq. (15) in the moving frame as

$$\frac{dn_p}{d\chi} = \frac{v_\phi}{\omega_p}\left(1-\frac{1}{\gamma_e{}^2}\right)^{1/2}\left(1-\frac{1}{\gamma_\phi{}^2}\right)^{-1/2} N_0 N_e \sigma_T, \quad (17)$$

where we used the definition of γ_e. Here

$$\gamma_\phi = 1/\sqrt{1-\frac{v_\phi^2}{c^2}},$$

N_e is given by Eq. (14), and $N_i = N_0$, because the ions are at rest.

4. NUMERICAL RESULTS

Equations (12), (13), and (17) are solved numerically and the results analyzed for different laser intensities (a_0), pulse widths (d), and directions of the external magnetic field ($\mathbf{\Omega}$). In all cases, we assume $\gamma_\phi \gg 1$,

$$\Psi = \frac{d\Psi}{d\chi} = 0$$

at infinity, and that the plasma is initially at rest.

For small values of a_0 (nonrelativistic regime), the optimum pulse width for wake generation is about half the plasma wavelength, as expected [14]. In this case of relatively weak laser intensity, the laser pulse induces sinusoidal wake oscillations typical of linear waves. As a_0 increases, the charge separation field and the wake potential also increase. However, to optimize the process, it is necessary to shorten the pulse width because the intensity of the ponderomotive force affects the charge separation field.

As the laser intensity increases, the eletric field of the excited plasma wave slowly grows and soon reaches the relativistic wave-breaking field for the given plasma density,

$$E_{WB} \approx 1.36\left[(\gamma_\phi - 1)\, N_0\right]^{1/2} \text{ V/cm},$$

(see [18]). Wave-breaking occurs at very large plasma wave amplitudes, when the wave motion becomes so nonlinear that the wave energy is converted directly into the particle kinetic energy [19]. The nonlinearity of the strong wakefield causes the steepening of the wave and the formation of localized maxima in the electron density, viz. the «spikes» [20]. This is characteristic of the wave-breaking regime, where the electrons are accelerated to speeds close to v_ϕ ($\gamma_e \to \gamma_\phi$) [21]. According to Eq. (1), which is given in a moving frame in (14), the electron density is given by

$$N_e = \frac{N_0 v_\phi}{v_\phi - v_e}$$

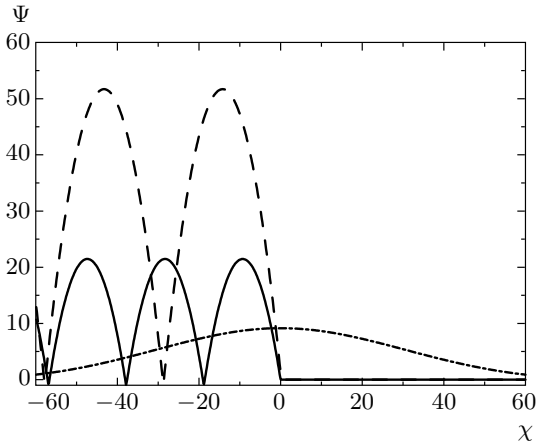

Fig. 1. The normalized potential Ψ for $B_0 = 0$ and $N_0 = 10^{10}$ cm^{-3}, $a_0 = 30$ and $d = 0.01\lambda_p$ (solid line), $0.03\lambda_p$ (dashed line) and $8\lambda_p$ (dot-dashed line)

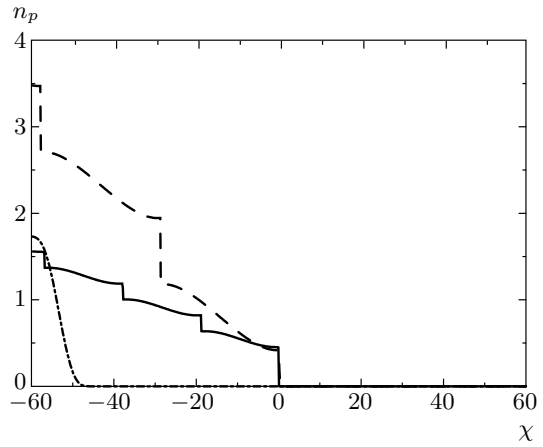

Fig. 2. The electron–positron pair concentration n_p (in unities of 10^9) for $B_0 = 0$ and $N_0 = 10^{19}$ cm^{-3}, $a_0 = 30$ and $d = 0.01\lambda_p$ (solid line), $0.03\lambda_p$ (dashed line) and $8\lambda_p$ (dot-dashed line)

for $v_{e_0} = 0$. Because the electron velocity v_e can vary from $-v_\phi$ to v_ϕ, the electron density varies from the minimal value $N_0/2$ to infinity (integrable).

For $B_0 = 0$, our results are in agreement with that found by Yu et al. [15] and by Krasovitskii et al. [22]. In this case, the perpendicular electron momentum is conserved,

$$\mathbf{P}_{e\perp} = \mathbf{P}_{ex} + \mathbf{P}_{ey} = \mathbf{a},$$

and the plasma electrons can acquire relativistic velocities as the laser intensity increases. For $N_0 = 10^{-4}$ cm^{-3}, $a_0 = 2$, $d = 0.35\lambda_p$ (the optimum pulse width for this laser intensity) and $d = 0.05\lambda_p$, the results agree with that found in Ref. [15]. The case $d = 0.05\lambda_p$ corresponds to direct electron acceleration by the laser, and the electron momentum and density become nearly synchronized with the pulse (however, weak wake oscillations are still excited). We found similar results for $d = 5\lambda_p$: in both cases, the laser pulse traps the electrons and carries them as a soliton-like system, accelerating them in the perpendicular direction. For all these parameters, the number of produced pairs is insignificant.

As the laser intensity increases, the excited wakefield grows and reaches the wave-breaking limit, but the number of produced pairs remains extremely small. Figure 1 displays the normalized potential Ψ for $a_0 = 30$ (corresponding to the laser intensity 10^{21} W/cm^2 for $\lambda = 1\mu$m), $N_0 = 10^{10}$ cm^{-3}, and three different values of $d = 0.01\lambda_p$, $0.03\lambda_p$, and $8\lambda_p$. For $d = 0.01\lambda_p$ and $0.03\lambda_p$, the electrons are accelerated by the generated wakefield in the z-direction, but for $d = 8\lambda_p$, the electrons are trapped and carried by the pulse. As the plasma density N_0 is increased, we observe that this parameter has small impact on the wakefield, but has an important effect on the pair concentration, as we see in Fig. 2. The values obtained for n_p agree with that in Ref. [10], and the «jumps» are here explained by a rapid increase in the electron density and energy at the points where the electric field is steeper and the potential is minimum in the wakefield [10]. We observe that for $d = 8\lambda_p$, the number of produced pairs saturates; in this case, the electrons are accelerated by the ponderomotive force of the laser and then produce pairs by scattering on the nuclei of the ions. For $d = 0.03\lambda_p$, near the optimum pulse width, the pair production reaches its maximum value, but it can be higher if the plasma is initially moving.

When the external magnetic field $\mathbf{B}_0$ is parallel to the direction of the pulse propagation, viz. $\mathbf{\Omega} = \omega_c\hat{z}$, none of the electron momentum components is conserved. In this case, we observe that for short pulses (d near or smaller than the optimum pulse width), the amplitudes of the normalized potential (and the pair concentration) grow as the strength of $\mathbf{B}_0$ increases up to a critical value. This limit value decreases as a_0 becomes lower. For larger values of d, the observed behavior is completely different: the increase of the magnetic field strength inhibits the particle acceleration by the wakefield and by the pulse, and consequently n_p diminishes as the parameter ω_c/ω_p increases. Figures 3 and 4 exhibit Ψ and n_p for the same parameters as in Figs. 2 and 3 for $\omega_c/\omega_p = 10$.

For $\mathbf{B}_0 = B_0\hat{x}$ (i.e. $\mathbf{\Omega} = \omega_c\hat{x}$), the component of

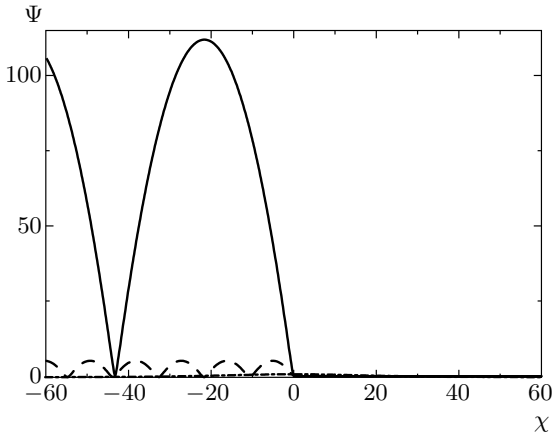

Fig. 3. The normalized potential Ψ for $\mathbf{B}_0 = B_0\hat{z}$ and $\omega_c/\omega_p = 10$, $N_0 = 10^{19}$ cm^{-3}, $a_0 = 30$ and $d = 0.01\lambda_p$ (solid line), $0.03\lambda_p$ (dashed line) and $8\lambda_p$ (dot-dashed line)

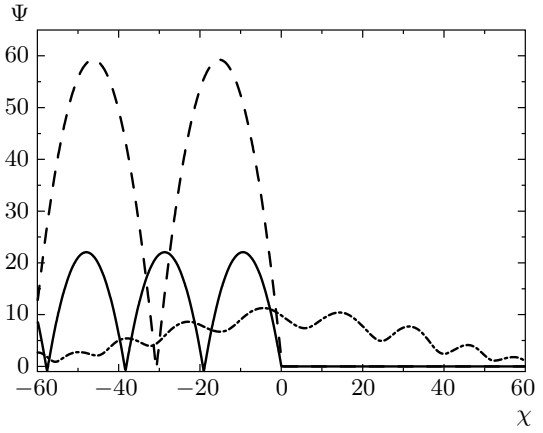

Fig. 5. The normalized potential Ψ for $\mathbf{B}_0 = B_0\hat{x}$ and $\omega_c/\omega_p = 1$, $N_0 = 10^{19}$ cm^{-3}, $a_0 = 30$ and $d = 0.01\lambda_p$ (solid line), $0.03\lambda_p$ (dashed line) and $8\lambda_p$ (dot-dashed line)

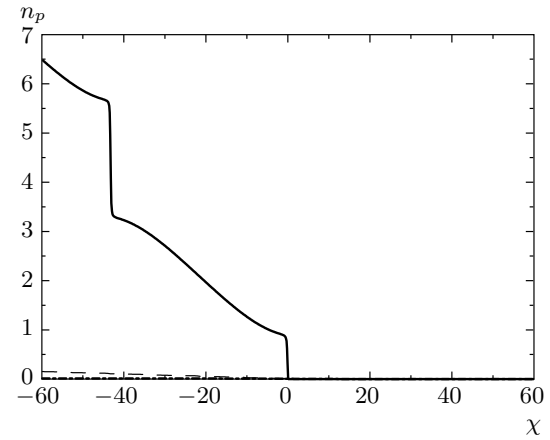

Fig. 4. The electron–positron pair concentration n_p (in unities of 10^9) for $\mathbf{B}_0 = B_0\hat{z}$ and $\omega_c/\omega_p = 10$, $N_0 = 10^{19}$ cm^{-3}, $a_0 = 30$ and $d = 0.01\lambda_p$ (solid line), $0.03\lambda_p$ (dashed line) and $8\lambda_p$ (dot-dashed line)

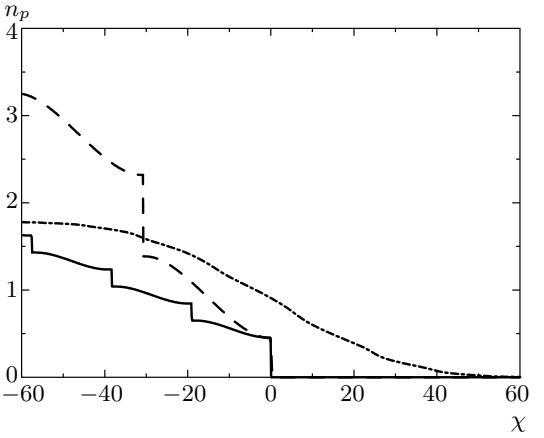

Fig. 6. The electron–positron pair concentration n_p (in unities of 10^9) for $\mathbf{B}_0 = B_0\hat{x}$ and $\omega_c/\omega_p = 1$, $N_0 = 10^{19}$ cm^{-3}, $a_0 = 30$ and $d = 0.01\lambda_p$ (solid line), $0.03\lambda_p$ (dashed line) and $8\lambda_p$ (dot-dashed line)

electron momentum parallel to the external magnetic field is conserved, $\mathbf{P}_e = \mathbf{a}_x$, as could be expected because the movement in this direction is not affected by the external magnetic field. We observe that for any values of a_0, d, and N_0, the wakefield grows up to a critical point and then decreases as the strength of the magnetic field increases. For widths near the laser optimum width, this critical point is very close to the resonance, when $\omega_c = \omega_p$; for others values of d, the critical point occurs for a higher parameter ω_c/ω_p. In Fig. 5, we see the increase of the wakefield for large values of d (dot-dashed curve). In this case, the wake field is more efficient in accelerating particles than the laser pulse, and then the jumps in pair concentration appear once more (see Fig. 6).

5. SUMMARY AND CONCLUSIONS

In this paper, we have studied electron–positron pair creation via the trident process, where the primary electrons are accelerated during laser–plasma interactions in the presence of an external magnetic field. We have worked at the wave-breaking regime, which has a characteristic of the formation of spikes in the elec-

tron density. At this limit, the electrons can be accelerated to relativistic speeds, where $\gamma_e \to \gamma_\phi$. The fast electrons can be scattered off in the Coulomb potential of stationary positive ions, thereby producing electron–positron pairs. The presence of an external magnetic field parallel to the direction of the laser pulse propagation inhibits the formation of the wakefield for long laser pulses and, consequently, the pair production. The situation is different for short laser pulses, where the wakefield is amplified by the external magnetic field until a critical value of B_0 is reached. When the external magnetic field is perpendicular to the laser pulse propagation direction, there is a considerable increase in the intensity of the generated wakefields for $\omega_c \approx \omega_p$ (for widths close to the optimum value), but as the magnetic field strength increases, both E and n_p decrease.

In conclusion, we emphasize that an efficient laboratory pair-production scheme depends on the development of the plasma-based wakefield electron accelerators that can supply the appropriate environment for a controlled pair production. Furthermore, our results should also be useful for understanding the origin of the electron-positron pairs in astrophysical settings (e.g., neutron stars and magnetars) involving intense electromagnetic waves and extremely high magnetic fields.

This work was partially supported by CAPES (Coordenadoria de Apoio ao Pessoal do Ensino Superior), Brazil, and by the Centre for Fundamental Physics at the Rutherford Appleton Laboratory, Chilton, Didcot, United Kingdom.

REFERENCES

1. J. Schwinger, Phys. Rev. **82**, 664 (1951).
2. Y. Kluger, J. M. Eisenberg, B. Svetitsky, F. Cooper, and E. Mottola, Phys. Rev. Lett. **67**, 2427 (1991).
3. V. S. Popov, Phys. Lett. A **298**, 83 (2002).
4. V. S. Popov, Zh. Eksp. Teor. Fiz. **121**, 1235 (2002).
5. S. V. Bulanov, T. Esirkepov, and T. Tajima, Phys. Rev. Lett. **91**, 085001 (2003); S. S. Bulanov, A. M. Fedotov, and F. Pegoraro, Pis'ma v Zh. Eksp. Teor. Fiz. **80**, 734 (2004).
6. S. S. Bulanov, Phys. Rev. E **69**, 036408 (2004); N. B. Narozhny, S. S. Bulanov, V. D. Mur, and V. S. Popov, Phys. Lett. A **330**, 1 (2004).
7. M. Mittleman, Phys. Rev. A **35**, 4624 (1987).
8. F. V. Bunkin and A. E. Kazakov, Dokl. Akad. Nauk SSR **193**, 1274 (1970).
9. J. W. Shearer, J. Garrison, J. Wong, and J. E. Swain, Phys. Rev. A **8**, 1582 (1973).
10. V. I. Berezhiani, D. D. Tskhakaya, and P. K. Shukla, Phys. Rev. A **46**, 6608 (1992).
11. L. A. Rios, A. Serbeto, J. T. Mendonça, P. K. Shukla, and R. Bingham, Phys. Lett. B **606**, 79 (2005).
12. V. I. Berezhiani, D. P. Garuchava, S. V. Mikeladze, K. I. Sigua, N. L. Tsintsadze, S. M. Mahajan, Y. Kishimoto, and K. Nishikawa, Phys. Plasmas **12**, 062308 (2005).
13. M. Tatarakis, I. Watts, F. N. Beg et al., Nature **415**, 280 (2002); U. Wagner, M. Tatarakis, A. Gopal et al., Phys. Rev. E **70**, 026401 (2004).
14. T. Tajima and J. M. Dawson, Phys. Rev. Lett. **43**, 267 (1979); T. Katsouleas and J. M. Dawson, ibid. **51**, 392 (1983): R. Bingham, J. T. Mendonça, and P. K. Shukla, Plasma Phys. Control. Fusion **46**, R1 (2004).
15. M. Y. Yu, W. Yu, Z. Y. Chen, J. Zhang, Y. Yin, L. H. Cao, P. X. Lu, and Z. Z. Xu, Phys. Plasmas **10**, 2468 (2003).
16. D. Umstadter, Phys. Plasmas **8**, 1774 (2001).
17. W. Heitler, *The Quantum Theory of Radiation*, Clarendon, Oxford (1954).
18. E. Esarey and P. Sprangle, IEEE Trans. Plasma Sci. **24**, 252 (1996).
19. S. P. D. Mangles et al., Nature **431**, 535 (2004).
20. A. I. Akhiezer and R. V. Polovin, Sov. Phys. JETP **30**, 915 (1956).
21. S. V. Bulanov et al., in Reviews of Plasma Physics, ed. by V. D. Shafranov, Kluwer Academic/Plenum Publishers, New York (2001), Vol. 22, p. 227.
22. V. B. Krasovitskii, V. G. Dorofeenko, V. I. Sotnikov, and B. S. Bauer, Phys. Plasmas **11**, 724 (2004).